

Supplemental Table 1. Candidate genes discovered from the functional screen

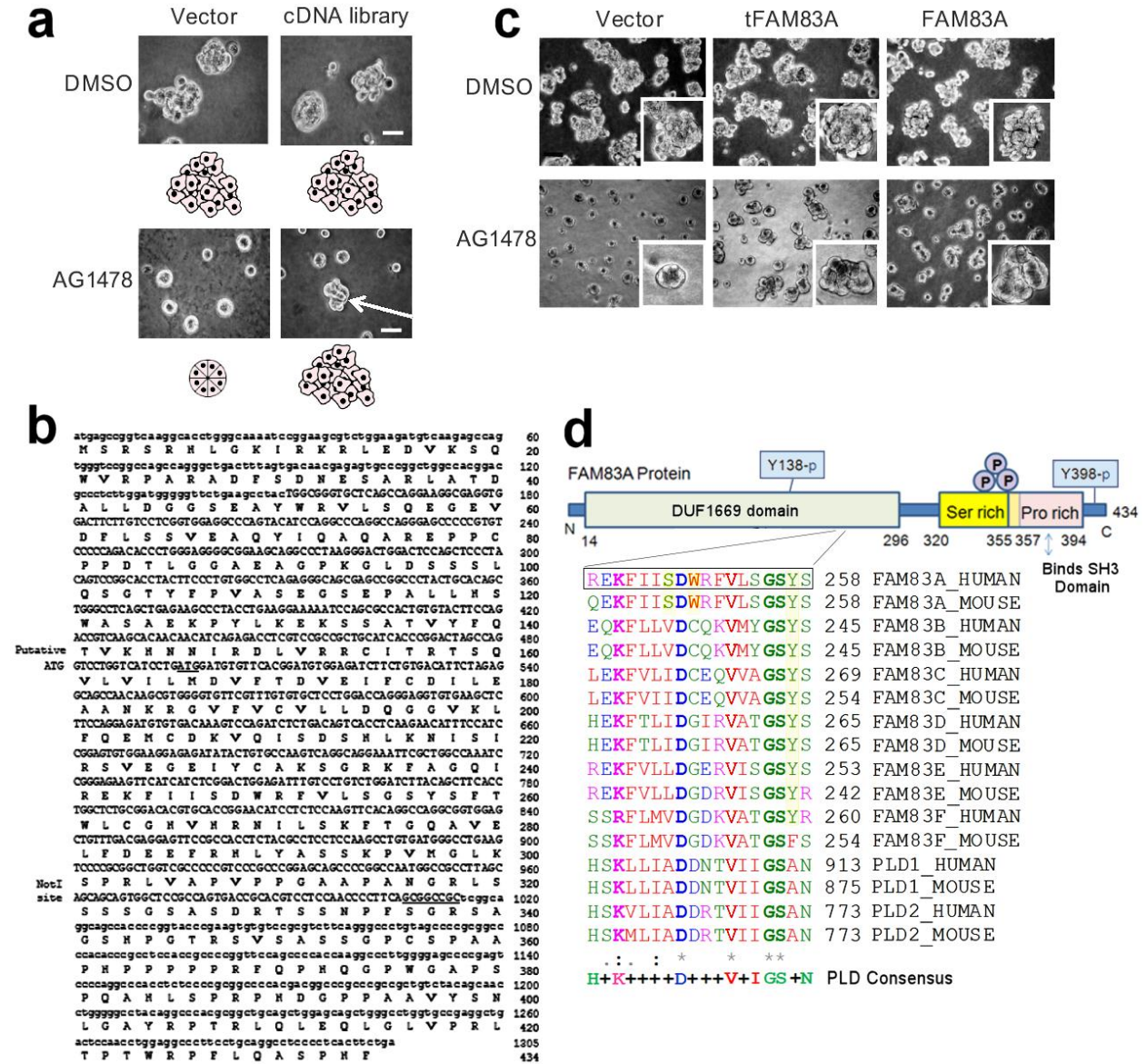
Gene Name	Accession No.	Remarks	Locus	Resistance
Hypothetical protein LOC84985	NM207006	Hypothetical, contains phospholipase D active domain	8q24.13	AG1478 (EGFR)
MRG(MORF4-related gene)-binding protein (MRGBP)	NM018270	Chromatin modification, regulation of transcription, regulation of cell growth	20q13.33	LY294002 (PI3K)
Zinc-finger protein like 1 (ZFPL1)	NM006782	Zinc ion binding, integral to membrane, biological process is unknown	11q13	Ly294002 (PI3K)
Polypyrimidine tract binding protein variant 1 (PTBP1)	NM002819	hnRNPs:RNA binding protein, pre-mRNA processing, mRNA metabolism and transport	19p13.3	Ly294002 (PI3K)
Rab32	NM006834	Ras family, Rab GTPase, a kinase anchoring protein, mitochondria dynamics	6q24.3	AG1478 (EGFR)

Supplemental Table 2. Cell lines used for the analysis in **Supplemental Fig. 7 (1)**.

Cell.line	GEO.ID	Histology	Set	EGFR	KRAS	IC50.umol.L	FAM83A.expression
H3255	GSM99018	Adenocarcinoma	Mutant	Mutant	NA	0.015	9.23325385
A549	GSM99019	Adenocarcinoma	Train	Wild-type	Wild-type	9.6	8.562611441
Calu3	GSM99020	Adenocarcinoma	Train	Wild-type	NA	0.3	7.438812196
H125	GSM99021	Adenosquamous	Train	Wild-type	Wild-type	4.8	9.179826983
H1334	GSM99022	Large	Train	Wild-type	Wild-type	0.3	8.073124457
H157	GSM99023	Squamous	Train	Wild-type	Mutant	12.8	8.683971565
H157	GSM99023	Squamous	Test	Wild-type	Mutant	13.8	8.683971565
H1648	GSM99024	Adenocarcinoma	Train	Wild-type	Wild-type	0.38	9.606765642
H1650	GSM99025	Adenocarcinoma	Mutant	Mutant	Wild-type	1	9.462717022
H1703	GSM99026	Squamous	Train	Wild-type	Wild-type	8	7.57965065
H1975	GSM99027	Adenocarcinoma	Mutant	Mutant	Wild-type	8	9.735347065
H358	GSM99030	BAC	Train	Wild-type	Mutant	0.18	9.156481553
H460	GSM99031	Large	Train	Wild-type	Mutant	12.9	8.504351252
H460	GSM99031	Large	Test	Wild-type	Mutant	8	8.504351252
H520	GSM99032	Squamous	Train	Wild-type	NA	13.6	7.552893222
H820	GSM99033	Adenocarcinoma	Mutant	Mutant	Wild-type	3	8.836597887
HCC4006	GSM99034	Adenocarcinoma	Mutant	Mutant	Wild-type	0.02	8.178024513
HCC827	GSM99035	Adenocarcinoma	Test	Mutant	Wild-type	0.005	8.33929926

Supplemental Figures

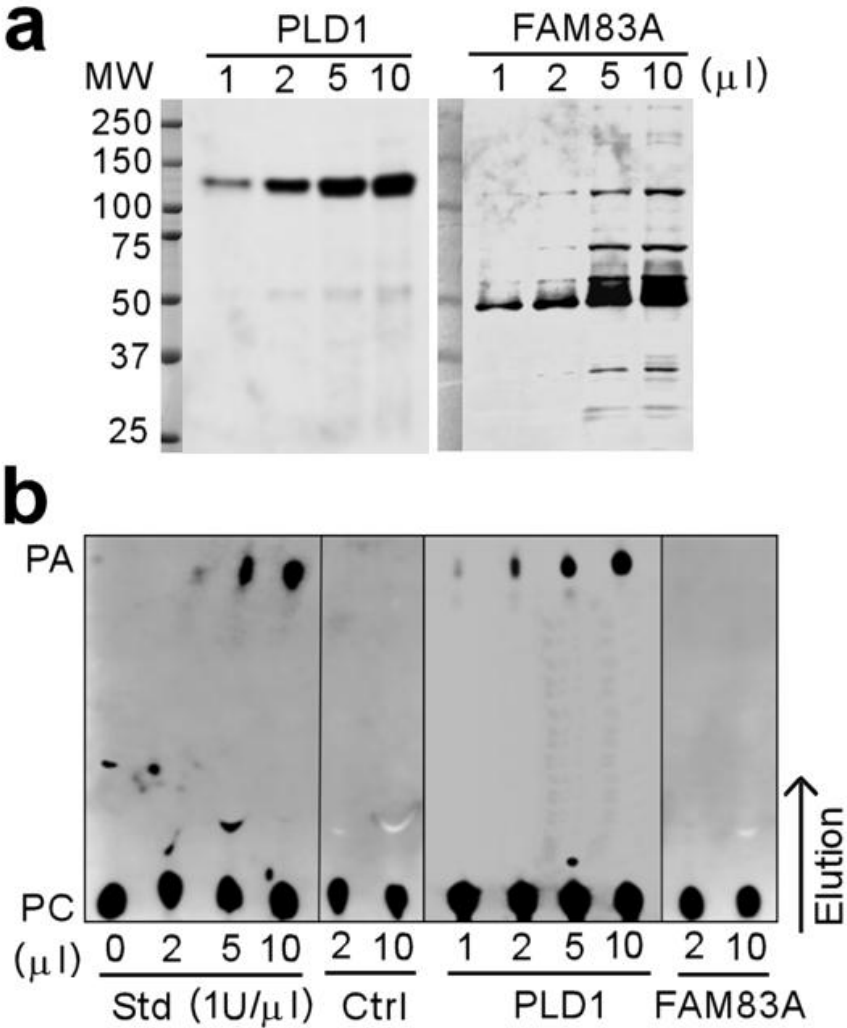
Supplemental Figure 1



Supplemental Figure 1. Overexpression of the truncated or full length FAM83A renders T4-2 cells resistant to AG1478-induced phenotypic reversion in 3D cultures.

(a) cDNA library-transduced T4-2 cells were treated with 100nM AG1478 in 3D IrECM for 4 days. Colonies that displayed resistance to reversion (black arrow) were isolated (scale bar: 50 μ m). (b) Full-length DNA and amino acid sequences of FAM83A. Capitalized DNA sequence represents those obtained in the initial clone. (c) Full-length or truncated FAM83A-overexpressing T4-2 cells in the absence (top) or presence (bottom) of the EGFR inhibitor, AG1478 (scale bar: 50 μ m). (d) Schematic for the protein domain structure of FAM83A. The regions containing the PLD consensus-like motif are aligned among different FAM83 family members in relation to PLD1 and PLD2.

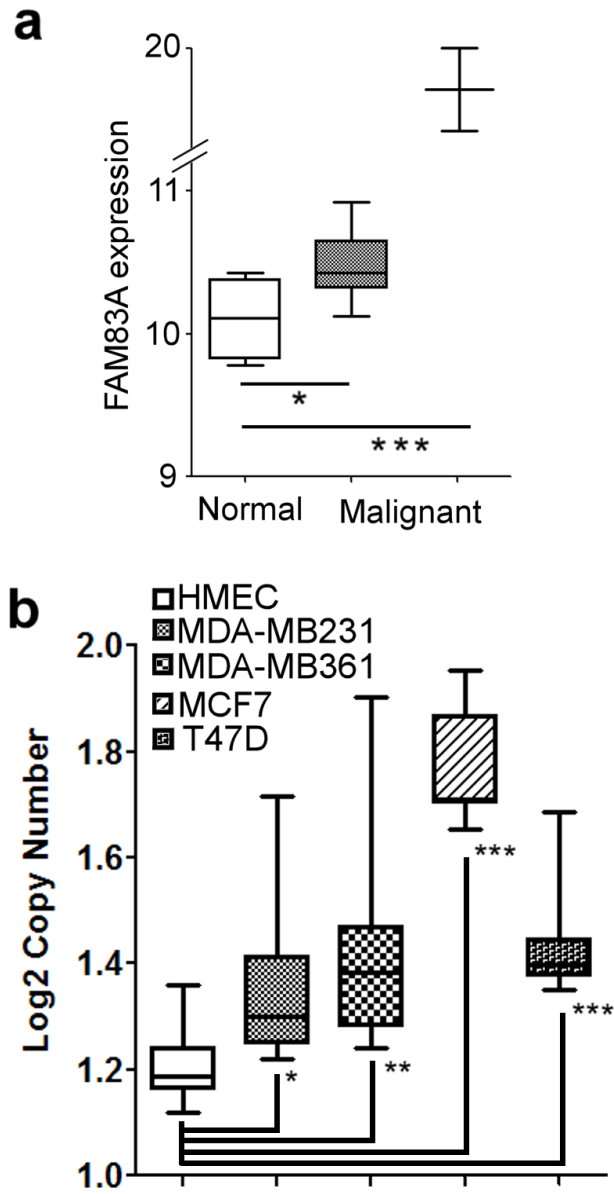
Supplemental Figure 2



Supplemental Figure 2. FAM83A protein prepared by *in vitro* transcription/translation does not exhibit detectable phospholipase D activity measured by thin layer chromatography.

(a) Human phospholipase D1 (PLD1, MW= 124 kDa, left) and FAM83A (MW= 49 kDa, right) proteins prepared by *in vitro* transcription/translation of PLD1- and FAM83A-expressing plasmids were analyzed by western blot. (b) Phospholipase D protein standard (Std) and *in vitro* transcription/translation products prepared from empty vector (Ctrl), PLD1-expressing plasmid (PLD1), and FAM83A-expressing plasmid (FAM83A) were incubated with phosphatidylcholine substrate (PC) for 90 min at 30 °C. The reaction product was separated by thin layer chromatography, and phospholipase D activity was detected by the presence of the faster migrating phosphatidic acid (PA) as the cleavage product.

Supplemental Figure 3

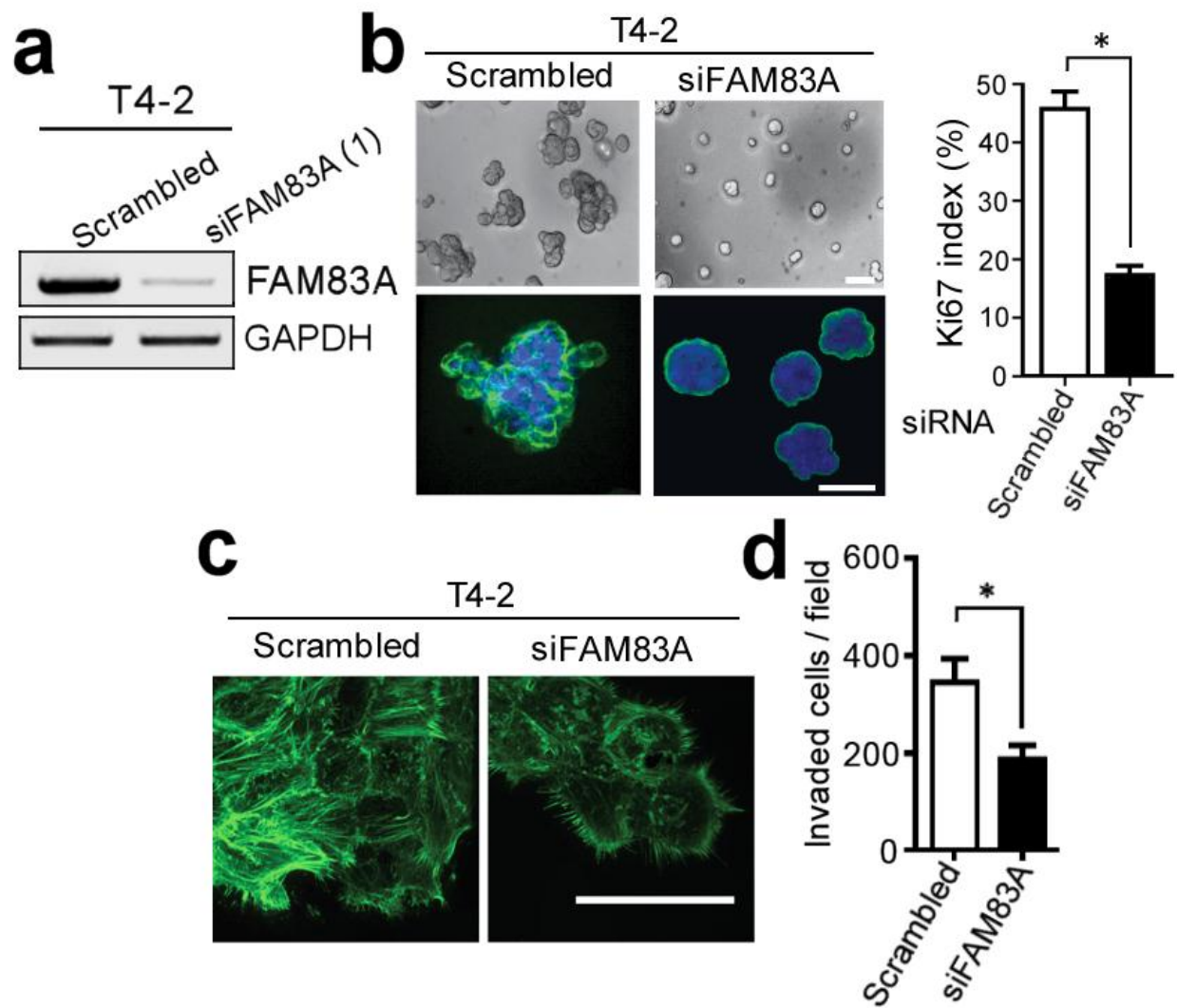


Supplemental Figure 3. FAM83A gene expression is upregulated and the gene locus is amplified in breast cancer.

(a) FAM83A gene expression in normal (n=4, first column) vs. cancerous (infiltrating ductal carcinoma; n=8, middle and n=2, right column [very high FAM83A expressers]) breast tissue samples. The analysis was performed on the dataset obtained from Howthorn et al. (GSE22840) (2). (Student's t-test: *p < 0.05, **p < 0.01, ***p < 0.001.

(b) FAM83A gene copy number in non-malignant (HMEC) vs. cancerous (Mda-MB231, MDA-MB361, MCF7, and T47D) breast cell lines. The analysis was performed on the datasets obtained from Beroukhim et al. (GSE19399) (3). (n= 13, Student's t-test: *p < 0.05, **p < 0.01, ***p < 0.001.)

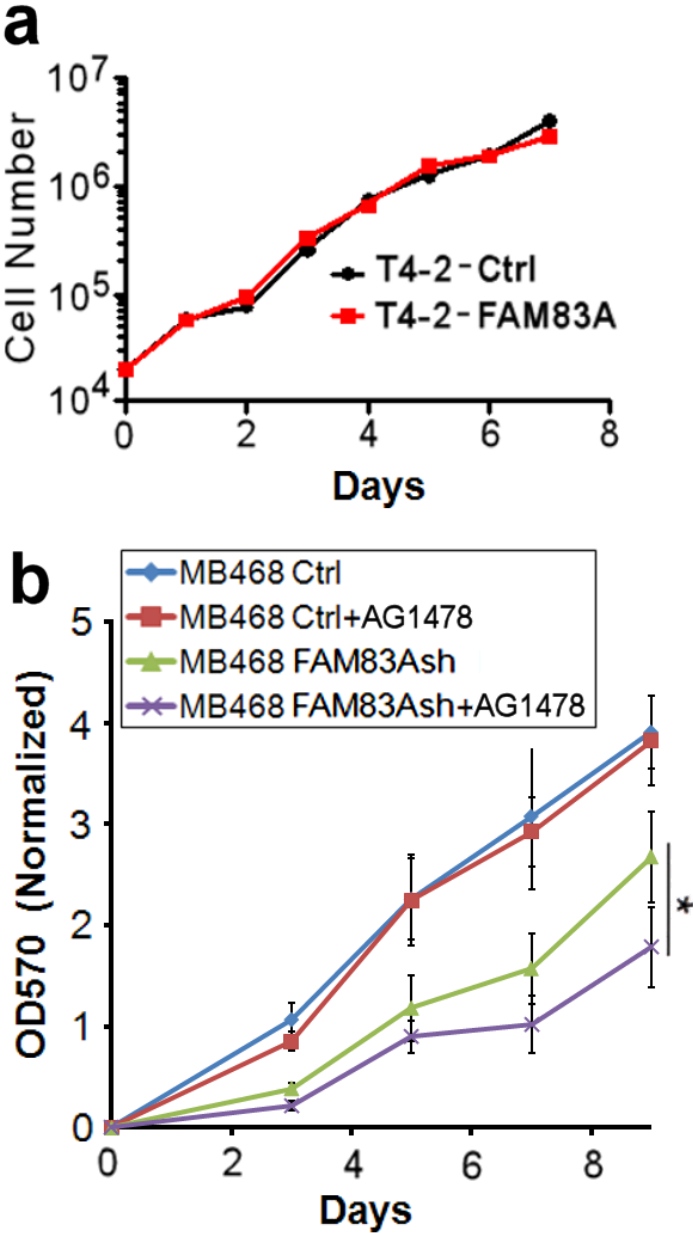
Supplemental Figure 4



Supplemental Figure 4. Reduction of FAM83A with specific siRNA impairs proliferative and invasive potentials of breast cancer cells.

(a) FAM83A siRNA treatment to deplete FAM83A expression in T4-2 cells. Two siRNAs were used and siRNA (1) gave more complete inhibition. (b) (Left) FAM83A siRNA treatment reverted T4-2 cells to a polarized phenotype in 3D IrECM cultures. Top: Images were captured with phase I. Bottom: $\alpha 6$ -integrin staining (green) was used to indicate basal polarity (blue: DAPI; scale bars: 50 μ m). (Right) Ki67 staining of control (scrambled siRNA) and FAM83A siRNA-treated cells to measure cell proliferation status (Student's t-test: * $p < 0.05$). (c) T4-2 cells transfected with scrambled or FAM83A siRNA were stained for F-actin with phalloidin (scale bar: 50 μ m). (d) T4-2 cells were treated with FAM83A siRNA vs. control (scrambled), and invaded cells through IrECM-coated transwell filters were counted after 48 hours (n=3; Student's t-test: * $p < 0.05$).

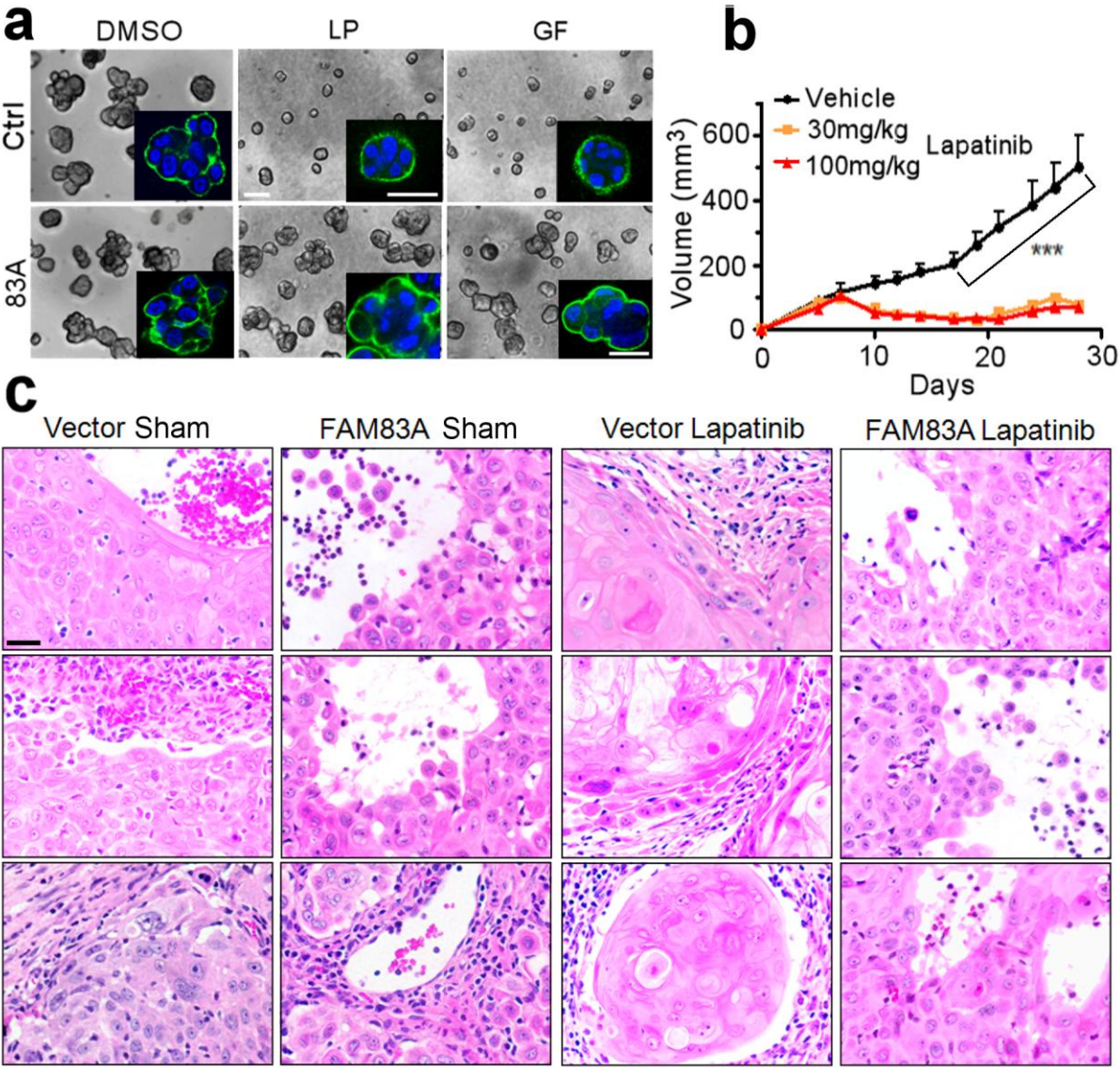
Supplemental Figure 5



Supplemental Figure 5. FAM83A expression does not accelerate cell growth, but confers resistance to EGFR-TKI.

(a) T4-2 cells expressing vector (Ctrl) or FAM83A constructs were grown for 7 days in 2D monolayer cultures and cell numbers were monitored. (b) Growth of vector control vs. FAM83A-depleted MDA-MB468 cells treated with vehicle or AG1478 (300 nM) and measured by MTT assay for a period of 9 days (n=12; ANOVA two-tailed test: *p<0.05).

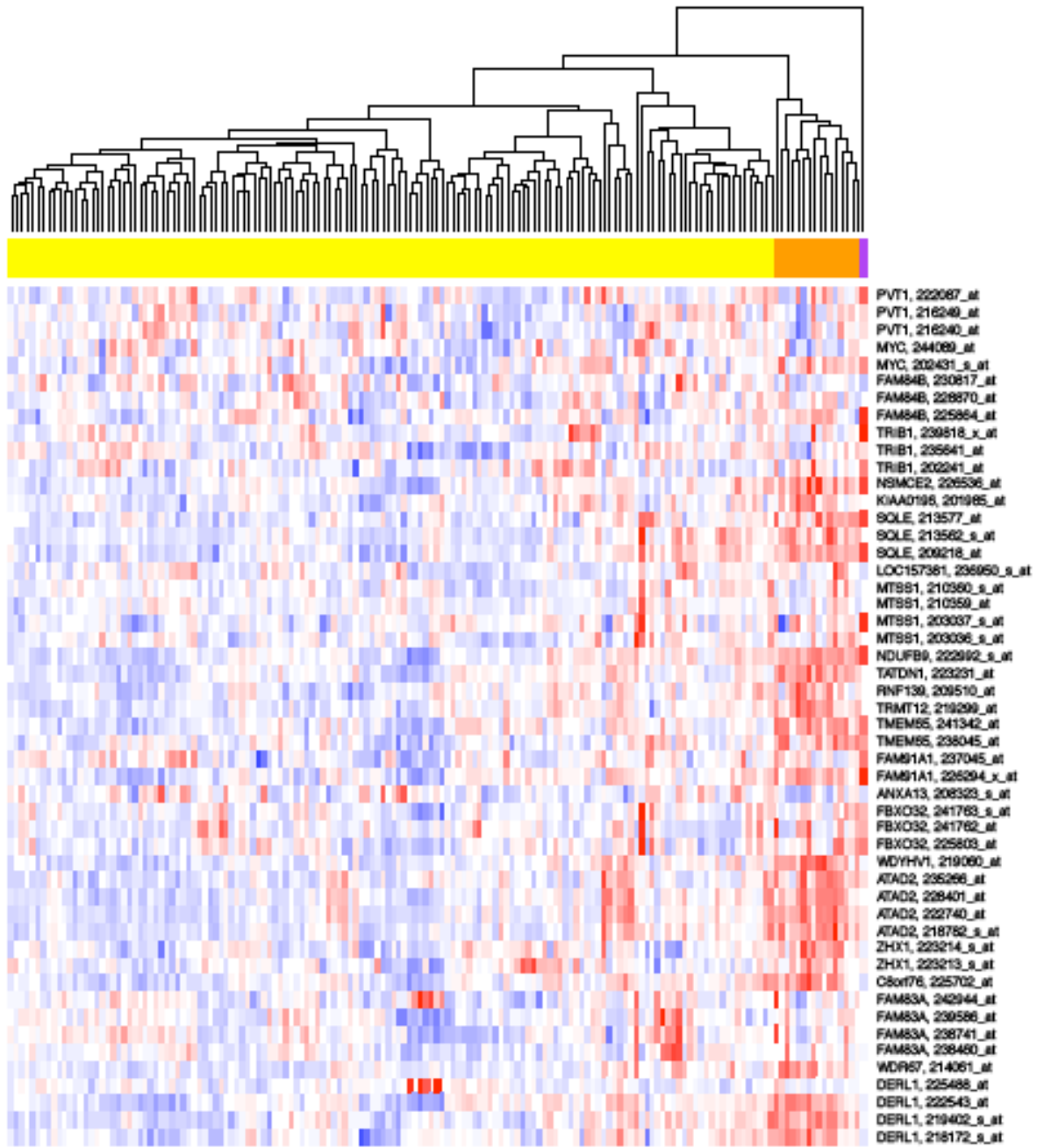
Supplemental Figure 6



Supplemental Figure 6. FAM83A overexpression confers resistance to tumor growth-suppressive activity of lapatinib in mice.

(a) Vector control vs. FAM83A-overexpressing T4-2 cells were tested for their response to lapatinib (LP) or genitinib (GF) in 3D IrECM culture. α 6-integrin staining (green) was used to indicate basal polarity (blue: DAPI; scale bars: 50 μ m). (b) Control T4-2 breast cancer cells were xenografted subcutaneously into nude mice. Mice were treated with vehicle or lapatinib (30 mg/kg or 100 mg/kg; n=8) using oral gavage for four weeks and tumor growth was monitored (2 way ANOVA analysis with Bonferroni post test: $p < 0.001$). Note the dose-independent tumor growth-suppressive activity of lapatinib. (c) H&E stained sections of tumors excised from mice at the end of the experiment described in **Figure 3b**. Note the well-circumscribed and little or no invasiveness phenotype of control (vector) tumors treated with lapatinib in comparison to lapatinib-treated FAM83A-overexpressing tumors. (scale bar: 50 μ m)

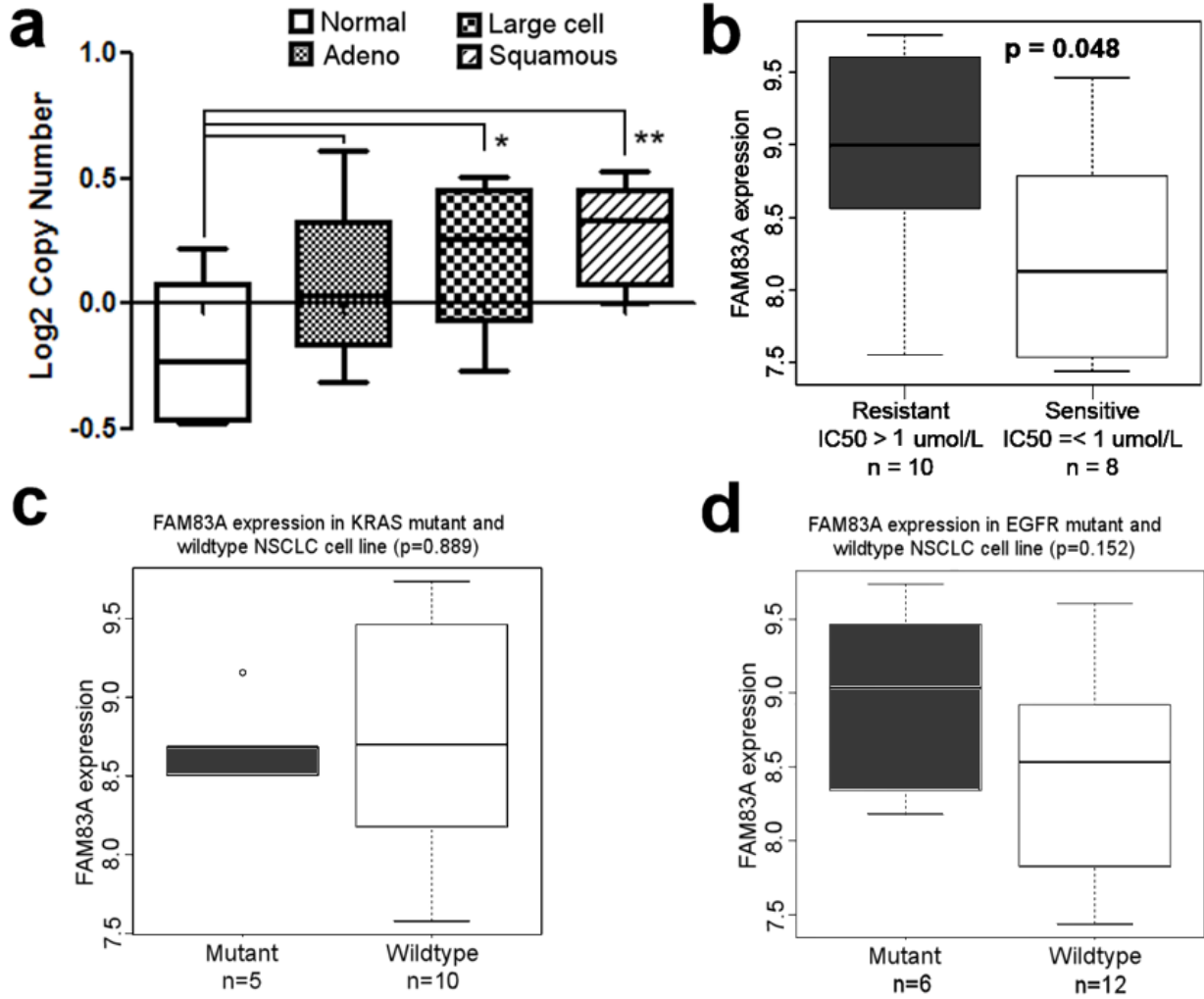
Supplemental Figure 7



Supplemental Figure 7. Hierarchical clustering of breast tumor samples by expression of genes located in the 8q24 amplicon.

A set of 24 genes located in 8q24 amplicon were used to cluster 159 breast cancer samples based on the expression level (red=high, blue=low). Clustering identified two main classes of tumors displaying either high (orange) or low (yellow) expression for genes in the 8q24 amplicon with a single outlier sample (purple). Rows: relative expression level of probe; Columns: individual tumor samples. Genes are organized from top to bottom based on their chromosomal position.

Supplemental Figure 8



Supplemental Figure 8. FAM83A gene is amplified in lung cancers and its overexpression correlates with resistance to EGFR-TKI.

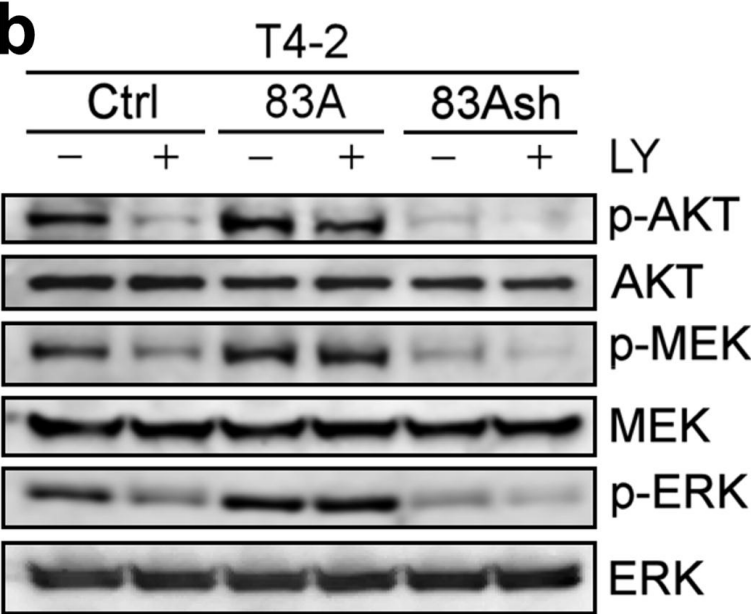
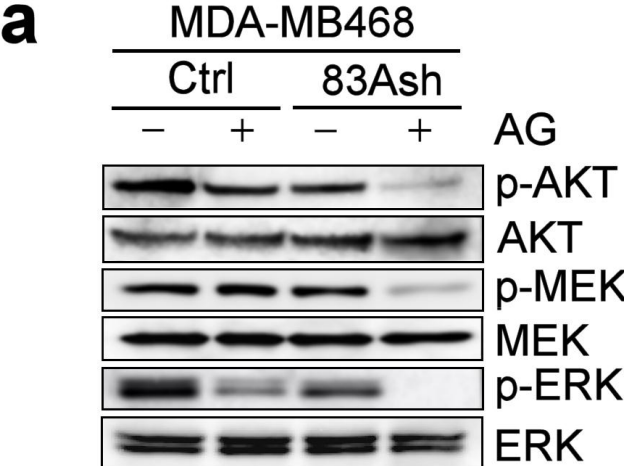
(a) FAM83A gene copy number in normal vs. cancerous lung tissues. The analysis was performed on the datasets obtained from Micke et al. (GSE28572)(4). Adeno: adenocarcinoma, Large cell: large cell carcinoma, and Squamous: squamous carcinoma. (n= 5. Student's t-test: *p < 0.05, **p < 0.01.

(b) FAM83A expression in non-small cell lung carcinoma cells that have become resistant vs. those sensitive to gefitinib treatment. The analysis was performed on the dataset obtained from Coldren et al. (GSE4342) (1). (Student's t-test: *p < 0.05.) See **Supplemental Table 2** for cell lines used for the analysis.

(c) FAM83A expression in non-small cell lung carcinoma cells is irrelevant to KRAS mutation status. The analysis was performed as in (b). (Student's t-test: p > 0.05.)

(d) FAM83A expression in non-small cell lung carcinoma cells is irrelevant to EGFR mutation status. The analysis was performed as in (b). (Student's t-test: p > 0.05.)

Supplemental Figure 9

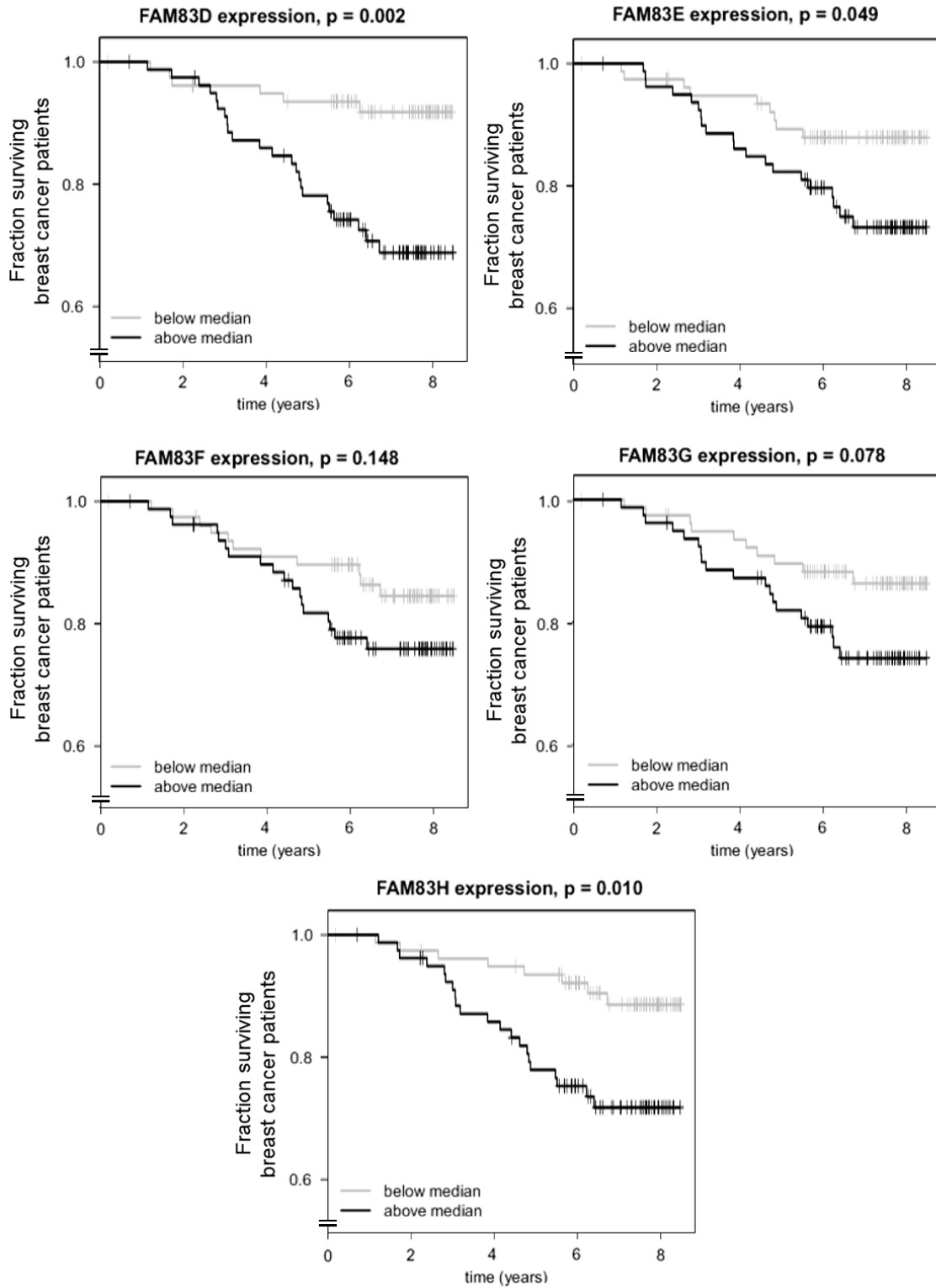


Supplemental Figure 9. FAM83A level dictates the degree of resistance to EGFR-TKI AG1478 and PI3K inhibitor LY294002.

(a) EGFR-TKI resistant breast cancer cell line, MDA-MB468, was treated with scramble (Ctrl) or FAM83Ash and cultured in the absence (-) or presence (+) of AG1478 for 2 hours. The levels of phosphorylated AKT, MEK1/2 and ERK1/2 were determined by western analysis.

(b) Control, FAM83A-overexpressing and FAM83Ash-expressing T4-2 cells were treated with LY294002 for 2 hours and the levels of phosphorylated AKT, MEK1/2 and ERK1/2 were determined by western analysis.

Supplemental Figure 10



Supplemental Figure 10. Correlation analysis for the expression of different FAM83 Family members (D,E, F, G and H) and breast cancer survival.

The results are shown in Kaplan-Meier curves for a cohort of 159 patient samples (above median expression level vs. below medium expression level of a different FAM83 member).

References

1. Coldren, C.D., Helfrich, B.A., Witta, S.E., Sugita, M., Lapadat, R., Zeng, C., Barón, A., Franklin, W.A., Hirsch, F.R., Geraci, M.W., et al. 2006. Baseline gene expression predicts sensitivity to gefitinib in non-small cell lung cancer cell lines. *Mol. cancer Res.* 48.
2. Hawthorn, L., Luce, J., Stein, L., and Rothschild, J. 2010. Integration of transcript expression, copy number and LOH analysis of infiltrating ductal carcinoma of the breast. *BMC cancer* 10:460.
3. Beroukhi, R., Mermel, C.H., Porter, D., Wei, G., Raychaudhuri, S., Donovan, J., Barretina, J., Boehm, J.S., Dobson, J., Urashima, M., et al. 2010. The landscape of somatic copy-number alteration across human cancers. *Nature* 463.
4. Micke, P., Edlund, K., Holmberg, L., Kultima, H.G., Mansouri, L., Ekman, S., Bergqvist, M., Scheibenflug, L., Lamberg, K., Myrdal, G., et al. 2011. Gene copy number aberrations are associated with survival in histologic subgroups of non-small cell lung cancer. *J Thorac Oncol.* 6:1833-1840.